Journal of Geophysical Research: Biogeosciences

RESEARCH ARTICLE
10.1029/2018JG004504

Key Points:
- Leaf photosynthesis and leaf respiration parameters contributed most to model output uncertainty
- Successional processes related to reproduction, competition, and mortality did not contribute more to model uncertainty at longer time frames
- Reducing the parameter uncertainty for processes controlling short-term carbon dynamics should be most effective at reducing long-term model predictive uncertainty

Supporting Information:
- Supporting Information S1

Correspondence to:
B. Raczka,
brett.raczka@utah.edu

Citation:
Raczka, B., Dietze, M. C., Serbin, S. P., & Davis, K. J. (2018). What limits predictive certainty of long-term carbon uptake? *Journal of Geophysical Research: Biogeosciences*, *123*, 3570–3588. https://doi.org/10.1029/2018JG004504

Received 21 MAR 2018
Accepted 25 OCT 2018
Accepted article online 19 NOV 2018
Published online 21 DEC 2018

What Limits Predictive Certainty of Long-Term Carbon Uptake?

Brett Raczka[1,2], Michael C. Dietze[3], Shawn P. Serbin[4], and Kenneth J. Davis[1]

[1]Department of Meteorology and Atmospheric Science, Pennsylvania State University, University Park, PA, USA, [2]Now at School of Biological Sciences, University of Utah, Salt Lake City, UT, USA, [3]Department of Earth and Environment, Boston University, Boston, MA, USA, [4]Environmental and Climate Sciences Department, Brookhaven National Laboratory, Upton, NY, USA

Abstract Terrestrial biosphere models can help identify physical processes that control carbon dynamics, including land-atmosphere CO_2 fluxes, and have the potential to project the terrestrial ecosystem response to changing climate. It is important to identify ecosystem processes most responsible for model predictive uncertainty and design improved model representation and observational system studies to reduce that uncertainty. Here we identified model parameters that contribute the most uncertainty to long-term (~100 years) projections of net ecosystem exchange, net primary production, and aboveground biomass within a mechanistic terrestrial biosphere model (Ecosystem Demography, version 2.1) ED2. An uncertainty analysis identified parameters that represent the quantum efficiency of light to photosynthetic conversion, leaf respiration and soil-plant water transfer as the highest contributors to model uncertainty regardless of time frame (annual, decadal, and centennial) and output (e.g., net ecosystem exchange, net primary production, aboveground biomass). Contrary to expectations, the contribution of successional processes related to reproduction, competition, and mortality did not increase as the time scale increased. These findings suggest that uncertainty in the parameters governing short-term ecosystem processes remains the most significant bottleneck to reducing predictive uncertainty. Key actions to reduce parameter uncertainty include more leaf-level trait measurements across multiple sites for quantum efficiency and leaf respiration rate. Further, the empirical representation of soil-plant water transfer should be replaced with a mechanistic, hydraulic representation of water flow, which can be constrained with direct measurements. This analysis focused on aboveground ecosystem processes. The impact of belowground carbon cycling, initial conditions, and meteorological forcing should be addressed in future studies.

Plain Language Summary Terrestrial biosphere models (TBMs) are used in climate modeling to predict exchanges of carbon dioxide, water, and energy between the land and atmosphere of the Earth. TBMs are important because they can predict the rate at which plants and the soils absorb or emit carbon dioxide to the atmosphere. The amount of carbon dioxide in the atmosphere determines the rate of climate warming. Because TBMs are an approximation of the true land processes it is important to estimate the amount of uncertainty within the model projections. Here we conduct an uncertainty analysis that identifies two model components that contribute the most to model uncertainty: the efficiency at which light energy is converted to photosynthesis and the rate at which leaves emit carbon dioxide. We recommend that more leaf-level measurements be taken across multiple sites so that we better understand these two processes and reduce the uncertainty they add to model projections.

1. Introduction

The terrestrial biosphere is responsible for the uptake of 30% of anthropogenic carbon emissions, which helps to mitigate the increase of atmospheric CO_2 and slow climate change (Le Quéré et al., 2018). It is uncertain, however, how much longer the terrestrial biosphere will maintain this level of service (Arora et al., 2013; Friedlingstein et al., 2014). Climate prediction relies in part upon terrestrial biosphere models (TBMs), which can simulate global land carbon uptake by tracking fluxes and pools of carbon, water, thermal energy, and momentum between the land-atmosphere interface. Although TBM uncertainty stems from several sources including model parameters, initial conditions (e.g., soil and vegetation state), and model driver data (e.g., meteorological conditions), it has been demonstrated that ecosystem model parameters are one of the most significant contributors to TBM simulation uncertainty (Lin et al., 2011).

Ecosystem observations help define appropriate ranges to model parameters that improve TBM performance (e.g., Dietze et al., 2013). These observations include chamber gas-exchange measurements, eddy covariance

flux measurements (carbon, sensible, and latent heat flux; e.g., Braswell et al., 2005), aboveground and belowground biomass (e.g., Medvigy et al., 2009), leaf area and chemistry, and information on soil properties. Through the use of remote sensing data, many of these critical measurements for informing models are obtained regionally using active and passive remote sensing systems (Schimel et al., 2015; Shugart et al., 2015). The importance of constraining model parameters with data is supported by the relatively high performance of simple models (e.g., LOTEC and EC-MOD) used within a data assimilation framework (Keenan et al., 2012; Raczka et al., 2013). More recent studies have incorporated the biometric observation of annual woody increment, or carbon stocks, which has shown the capacity to constrain interannual to decadal processes (i.e., 5–20 years) when compared to observations of carbon fluxes alone (Ricciuto et al., 2011; Richardson et al., 2010).

Assimilated ecosystem observations, however, have limited impact upon reducing model uncertainty for longer time frames. For example, Weng and Luo (2011) showed that 10 years of observations (e.g., biomass pools, soil carbon pools, and soil respiration) assimilated into a TBM at the Duke FACE experiment only reduced forecasting uncertainty for a few decades; century-scale carbon cycle forecasts were not well constrained. Overall, relatively short-term ($<$20 years) eddy covariance flux measurements of net ecosystem exchange (NEE) reduce uncertainty at the subdaily to seasonal time frames but not interannual variations in net carbon exchange and storage (Braswell et al., 2005; Ricciuto et al., 2008). In general, TBM's have difficulty capturing interannual variation in carbon uptake observed at flux towers with or without data assimilation (Keenan et al., 2012; Raczka et al., 2013). An important step forward is to attribute model uncertainty to particular ecological processes across a range of time scales (e.g., interannual to centennial) to target specific areas that require model development and observational system studies. The implication is that the importance of ecosystem processes within a modeled system also reflects their importance in the real world (Pappas et al., 2013; Saltelli et al., 2000). Previous sensitivity analyses of TBM's have identified vegetation processes as the most important for simulating carbon cycle variables, especially processes related to photosynthesis (e.g., Lu et al., 2013; Pappas et al., 2013; D. Ricciuto et al., 2018; Sargsyan et al., 2014). One limitation of these studies is that they generally use uniform distributions of ecological process parameters, which could overestimate parameter and model uncertainty.

The ecoinformatics software Predictive Ecosystem Analyzer, (PEcAn, pecanproject.org, see section 2.5) provides a framework that combines the Biofuel Ecophysiological Traits and Yield (BETY, betydb.org, see section 2.5.1) plant trait database and a TBM to attribute predictive uncertainty to ecosystem processes. Specifically, this setup allows for (1) an ecosystem trait-based estimate of parameter uncertainty and (2) a method to attribute the parameter uncertainty to model output uncertainty (LeBauer et al., 2013). This software estimates parameter uncertainty through a Bayesian approach (section 2.5.1), that recognizes trait data is composed of multiple distributions (i.e., collected from different sites, conditions) reflecting the heterogeneous nature of ecosystem processes (Dietze, 2017a). Overall, the workflow design of PEcAn is amenable to an iterative approach where the attribution of parameter uncertainty motivates targeted field research that is subsequently entered into the trait database (Davidson, 2012). PEcAn and the Ecosystem Demography Model (ED2; Medvigy et al., 2009) have been coupled previously to parameterize and simulate tundra vegetation (Davidson, 2012), as well as biofuel crops, including switchgrass (LeBauer et al., 2013) and hybrid poplar (Wang et al., 2013). PEcAn and ED2 were also used in a cross-biome uncertainty analysis of 17 global plant functional types (PFTs; Dietze, Serbin et al., 2014), which identified *growth respiration*, *soil-plant water conductance*, *stomatal sensitivity*, *carbon mortality*, and *quantum efficiency* as contributing the most uncertainty to net primary productivity (NPP) predictions at timescales from 1 to 10 years. All of these ED2 uncertainty analyses were performed for short time periods ($<$20 years). It remains unclear how the importance of processes change for longer integration times for cohort-based models such as ED2 that link land surface dynamics with plant demography (Fisher et al., 2018).

In general, mechanisms that influence the fast physiological response of an ecosystem to environmental conditions (e.g., photosynthetic and respiration fluxes) should dominate carbon dynamics at short time scales, whereas mechanisms influencing succession (e.g., mortality, resource competition, and recruitment) should be expected to dominate at longer time scales. Within a TBM this suggests that fast physiological response parameters (e.g., V_{cmax}, *quantum efficiency*, *leaf respiration*, and stomatal sensitivity) should dominate the uncertainty for subdecadal time scales, whereas parameters that control competition and

successional processes (e.g., *mortality* and *reproduction carbon*) should be more important at the centennial time scale. This working hypothesis is consistent with previous short-term ED2 uncertainty analyses (<20 years) for forested ecosystems (e.g., Dietze, Serbin, et al., 2014; Wang et al., 2013) in which fast response parameters were most important. However, given the fact that long-lived trees are known to be highly sensitive to mortality rate (Caswell, 2001; Franco & Silvertown, 1996), the expectation is that these successional processes should become more important at long time scales. Furthermore, given that TBMs with demographic representation (e.g., ED2) and explicitly represent successional processes (e.g., mortality, competition, and recruitment) and are becoming more favored compared to big-leaf representations of canopies (Fisher et al., 2018), it is essential to perform analyses that can help to parameterize these models for long time scale simulations. Therefore, we ask three key questions: (1) what ecological processes are most important for projecting long-term carbon uptake?, (2) do the most important processes change as a function of time?, and (3) are processes that control fast ecosystem response versus the ecosystem successional state most impactful at short and long time scales respectively?

We performed this analysis at the Willow Creek site (*US-WCr*) in Northern Wisconsin (B. D. Cook et al., 2004), part of the Ameriflux network of sites within the Chequamegon Ecosystem-Atmosphere Study. To address the key questions, we performed an ensemble of ED2 model simulations at *US-WCr* to identify the ecological processes that contribute the most to model uncertainty according to model output (NEE, NPP, and aboveground biomass [AGB]) and simulation time (annual, decadal, and centennial). Furthermore, we addressed these questions while considering parameter heterogeneity (i.e., across site and treatment variation), which to our knowledge has not been addressed for any ecosystem model. These findings should help guide future observation system studies and model structural improvements that target ecosystem processes most prone to uncertainty.

2. Methods

The ED2 cohort-based representation of an ecosystem is described (section 2.1) followed by a description of the most influential ED2 parameters (section 2.2). Next, we describe how the forest composition (section 2.3) and atmospheric conditions (section 2.4) are prescribed. Finally, the steps necessary to attribute parameter uncertainty to model uncertainty are provided (section 2.5).

2.1. Ecosystem Demography Model (Version 2)

The Ecosystem Demography Model (ED2; Medvigy et al., 2009) simulates both the short- term ecosystem response to atmospheric conditions as well as the long-term evolution of the ecosystem state from resource competition. ED2 uses size- and age-structured vegetation dynamics to capture the competition that a cohort of trees (i.e., trees of identical PFT, biomass, and stem density) experience for light, nutrients, and other resources. Representation of this fine-scale competition is important for properly simulating successional growth and long-term carbon dynamics within a forest (Pacala & Deutschman, 1995), yet is unaccounted for in the more common *big-leaf* TBMs (Levin et al., 1997). ED2 tracks stand and landscape processes by modeling the dynamics of cohorts and patches (i.e., groups of cohorts with similar stand age). The evolution of each cohort (i.e., changes in stem density from mortality and disturbance and biomass from growth) is governed by the biological and physical processes represented in the model conditioned upon the size and age since last disturbance. Although tracking size structure to capture fine-scale dynamics of plants is not unique to ED2 (Fisher et al., 2018), ED2's methodology for tracking the landscape-scale distribution of the size-age class distribution allows for the efficient spatial scaling from the cohort to patch to regional scales.

The biological and physical processes represented within ED2 include plant ecophysiology and photosynthesis (Farquhar et al., 1980), soil biogeochemistry (Bolker et al., 1998; Parton et al., 1988), hydrology (Walko et al., 2000), and leaf phenology (Botta et al., 2000). These biophysical processes, in turn, influence the fluxes of carbon, surface energy, moisture, and momentum (Medvigy et al., 2009; Rogers et al., 2017). Although model complexity by itself is not a guarantee of model performance, ED2 has had success in simulating interannual variation in carbon uptake (Trugman et al., 2016), simulating forest growth for regions remote from the calibration sites (Medvigy et al., 2009; Medvigy & Moorcroft, 2012), and performing well within the North American Carbon Program Site Synthesis (Dietze & Moorcroft, 2011; Schwalm et al., 2010).

Table 1
List of Median Parameter Values for All Three Plant Functional Types (PFTs) Used Within the Simulation

Parameter name	Description	Units	Early hardwood	Mid hardwood	Late hardwood
Carbon balance mortality	Mortality from light competition	$year^{-1}$	3.50*	7.00*	20.0
Root turnover	Transfer rate of fine root to litter carbon pool	$year^{-1}$	0.691	0.681	0.673
Growth respiration	Fraction of assimilated carbon to growth respiration	$gC\ gC^{-1}$	0.351	0.351	0.351
Stomatal sensitivity	Controls stomatal response to environment changes	dimensionless	5.87	5.75	5.87
Root/Leaf carbon	Ratio of carbon allocated to fine roots/leaves	$gC\ gC^{-1}$	0.636	0.995	1.47
Recruitment carbon	Fraction of storage carbon allocated to recruitment	$gC\ gC^{-1}$	0.318	0.316	0.312
Labile carbon	Fraction of litter carbon allocated to labile carbon pool	$gC\ gC^{-1}$	0.79	0.79	0.49
Soil–plant water conductance	Measure of soil moisture stress	$m^2\ kg\ leaf^{-1}$	0.00496	0.00470	0.00474
Background mortality	Mortality from non resource- competition processes	$year^{-1}$	0.001	0.001	0.001
Specific leaf area	Leaf area per leaf mass	$m^2\ kg\ leaf^{-1}$	13.66	14.32	16.6
Leaf respiration	Controls rate of leaf maintenance respiration	$\mu mol\ CO_2\ m^{-2}\ s^{-1}$	1.32	0.50	1.97
Quantum efficiency	Rate at which radiation is converted to assimilated carbon	$\mu mol\ CO_2\ (\mu mol\ photon)^{-1}$	0.0577	0.0396	0.06*
V_{cmax}	Carboxylation rate of photosynthesis at 25 °C	$\mu mol\ CO_2\ m^{-2}\ s^{-1}$	39.65	41.64	44.8
Root respiration	Controls rate of fine root respiration	$\mu mol\ CO_2\ kg^{-1}\ s^{-1}$	8.34	8.34	8.31
Minimum height	Minimum height for plant reproduction	meters	5.00	5.00	5.00

Note. Refer to Figure 2. These median parameter values are based on the *posterior_re* parameter distribution estimated using a Bayesian meta-analysis approach (see section 2.5.1) that combines expert priors (Dietze, Serbin, et al., 2014) and trait data (Table S1). The *asterisk* indicates that the nominal parameter values were manually tuned to gain a reasonable distribution of successional PFTs for near present-day conditions (see section 2.5.2).

Although ED2 also simulates nitrogen, nutrient limitation is turned off for these simulations to reduce the complexity of the processes controlling carbon exchange and limit the parameters contributing to model uncertainty. Additional specifics of the model structure and operation have been described in detail elsewhere (Medvigy, 2006; Medvigy et al., 2009; Moorcroft et al., 2001). Here we focused on a mechanistic description tailored specifically to the parameters that were varied during the uncertainty analysis (section 2.2).

2.2. ED2 Parameter Description

The complete list of parameters varied in our sensitivity analysis (Table 1) was chosen because they (1) represented ecological processes that were important for previous uncertainty analyses with ED2 simulations (Dietze, Serbin, et al., 2014; LeBauer et al., 2013; Medvigy et al., 2009; Wang et al., 2013) and (2) were influential in preliminary long-term carbon sequestration simulations performed for this study. A parameter description is provided here (parameters listed *in italics*) with more details located in Text S1 in the supporting information or Rogers et al. (2017). Gross primary productivity (GPP) is represented by a standard enzyme-kinetic model, which describes a plant's demand for carbon as the minimum between the light limited (influenced by quantum efficiency) and enzyme limited reaction rate (influenced by V_{cmax}) during photosynthesis (Farquhar et al., 1980). The *quantum efficiency* is the maximum molar efficiency at which absorbed photosynthetically active radiation is converted into assimilated CO_2, whereas V_{cmax} controls the maximum rate of CO_2 assimilation performed by the Rubisco enzyme. Photosynthetic and transpiration rates are coupled through the leaf stomatal conductance (influenced by stomatal sensitivity) following the Leuning (1995) variant of the Ball-Berry model (Ball et al., 1987).

Photosynthesis and transpiration are limited by plant-soil water transport, which is calculated as the product of a *soil-plant water conductance parameter,* available groundwater, and fine root biomass. The water conductance parameter is an empirical attempt to estimate the resistance of water flow from the soil to leaf. If the water supply does not meet the canopy water demand, calculated based on the stomatal conductance and vapor pressure deficit, the GPP and transpiration are scaled down. The *specific leaf area* is the leaf surface area per unit mass of leaf carbon and determines the amount of leaf surface area available to absorb light for photosynthesis and for transpiration.

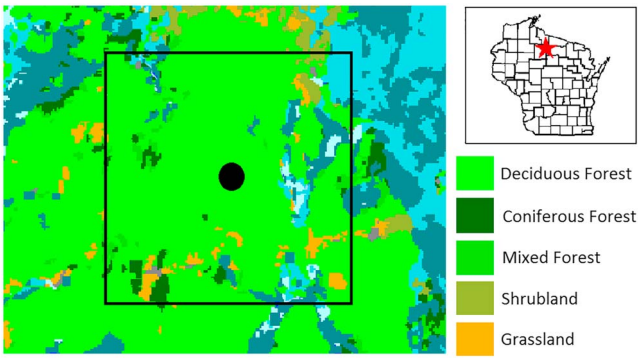

Figure 1. Vegetation land cover map centered on the coordinates of Willow Creek, Wisconsin (latitude: 45.81, longitude: −90.08, Ameriflux site: *US-WCr*), indicated by the black dot. The black box represents the 16-km^2 region from which the witness tree data observations were taken. This figure was created by data (~2000) and plotting tools available at: http://dnr.wi.gov/maps/gis/datalandcover.html. All blue shades represent wetland.

Plant (autotrophic) respiration is the sum of leaf maintenance respiration, root maintenance respiration, and growth respiration (all plant tissues). The leaf and root respiration is modeled as a function of respiration rate parameters (*leaf respiration* and *root respiration*), biomass, and temperature. The respiration required to support tissue growth is modeled as a fixed fraction (growth respiration) of the previous day's carbon balance. The *root turnover* parameter is a coefficient that determines the (turnover) rate at which fine roots are transferred to the litter pool. The *root/leaf carbon* parameter determines the fraction of the active biomass carbon pool (B_a) that is partitioned between roots and leaves, and assumes that these pools are always in a fixed ratio. If the active biomass carbon pool exceeds the allometric expectation based on cohort tree diameter, the excess carbon is assigned to a storage pool ($B_{storage}$). The amount of carbon used for reproduction (*reproduction carbon*) is the fraction of $B_{storage}$ that is allocated to reproduction (seed). The *minimum height* parameter defines the height of a tree before it can devote carbon to seed.

Tree mortality is calculated from disturbance-driven, hard freeze, carbon balance, and density independent contributions. Carbon-balance tree mortality is calculated as an exponentially decreasing function with a decay rate parameter (*carbon mortality*). The likelihood of carbon-balance mortality decreases as the cumulative carbon balance (sum of GPP, plant respiration, and litter fluxes) for a cohort approaches the maximum possible cumulative carbon balance (i.e., cohort at top of canopy). This is meant to account for shading competition between cohorts. The density independent mortality parameter (*background mortality*) is the background mortality rate in the absence of competition taking into account processes like wind and insect damage.

2.3. Site and Prescription of Initial Vegetation Conditions

All model simulations were performed at the Ameriflux site of Willow Creek (*US-WCr*) because it has a long-term flux record with considerable ancillary biological data and is representative of the larger region having experienced both climate change (Woods, 2000). In this way these findings should be applicable to a broader area across North America with similar ecosystem type. The site is a secondary deciduous broadleaf forest recovering from a 1930 clear-cut harvest and consists primarily of sugar maple, red oak, birch, and basswood tree species. Flux tower observations (Cook et al., 2004) have recorded carbon, sensible and latent heat fluxes since 1998. Both witness tree data (Liu et al., 2011) and a land cover data set developed by the Wisconsin Initiative for Statewide Cooperation on Landscape Analysis and Data (WISCLAND; Figure 1) were used to define the forest species composition (Figure S1), tree diameter, and stem density at the start of the model simulation during the year 1900. See Text S2 for more details. The soil carbon pools were initialized from contemporary observations of soil carbon located at the nearby, old growth, Sylvania Forest (Ameriflux site: *US-Syv*) in northern Wisconsin (Tang et al., 2009). It was assumed that the observed soil carbon at *US-Syv* is comparable to *US-WCr* (~1900) as both sites would, in 1900, have been old growth forests (>300 years since last disturbance).

2.4. Prescription of Atmospheric Conditions

We designed a custom meteorology product to perform the ED2 simulations that combined the multidecadal trends of Climate Research Unit, National Centers for Environmental Prediction (CRU-NCEP) meteorology product (1901–2010), with the site-level, high temporal resolution observations from the *US-WCr* (1998–2006; Ricciuto et al., 2013). We provided meteorological forcing to ED2 at 30-min resolution for air temperature, precipitation rate, wind speed, specific humidity, air pressure, longwave radiation, and shortwave radiation. The details of this method are provided in Text S3 and Figure S2. ED2 requires specific frequency bands of radiation to run; therefore, we used an algorithm (Weiss & Norman, 1985) to partition the total shortwave radiation into direct (visible and infrared) and diffuse (visible and infrared) components based upon the potential shortwave radiation from a cloudless sky as function of time of year, time of day, and location.

The monthly atmospheric CO_2 concentration time series at *US-WCr* was derived from the annual mean atmospheric CO_2 from both the Law Dome record (Etheridge et al., 1998) and Mauna Loa Observatory record (Thoning et al., 1989). The average seasonal cycle of atmospheric CO_2 as measured from the 1998–2006 flux tower records at *US-WCr* was added to the Law Dome/Mauna Loa record to estimate *US-WCr* atmospheric CO_2 from 1901 to 2010 (Figure S2).

2.5. Attributing Uncertainty to Ecological Processes

One way to quantify the influence of an ecosystem process upon carbon dynamics is through the attribution of ecosystem process parameter uncertainty to model output uncertainty. In practice, this is done by performing an ensemble of model simulations that spans the range of uncertainty for each process parameter (*parameter uncertainty*) and the range of the model solutions is an estimate of *model uncertainty*. The model uncertainty is a function of both the parameter uncertainty and the inherent *sensitivity* of the model to the parameter change. We used the Predictive Ecosystem Analyzer (PEcAn) ecoinformatics software version 0.3.2 (www.pecanproject.org) to calculate the parameter uncertainty as described in section 2.5.1. We then used that parameter uncertainty to organize and execute a series of ED2 simulations to calculate the *model sensitivity* and model uncertainty as described in section 2.5.2. A discussion of how parameter interactions may have contributed to model uncertainty is provided in section 2.5.3. To help simplify this analysis, only parameter uncertainty for the late hardwood PFT is considered as described in section 2.5.4.

2.5.1. Calculating Parameter Uncertainty

The parameter uncertainty was calculated based upon a library of independent, prior parameter distributions, and trait data available within the BETY database. These prior parameter distributions provided important information about the most likely parameter values, although the distributions were broad. Information about the prior distribution and trait data (when available) were combined using a Bayesian approach to estimate the posterior distribution for each parameter. The trait data (e.g., Table S1 in the supporting information; last access January 2014) were based upon field data or summary statistics collected from literature and are specific to a PFT (e.g., Bauer et al., 2001; Jose & Gillespie, 1996; Walters et al., 1993). In practice, trait data were not available for every parameter; therefore, parameters without trait data used the prior distributions to estimate parameter uncertainty.

To calculate the posterior distributions, PEcAn used the trait data and prior distributions to inform a linear mixed model for the unobserved *true* trait mean Θ_{ij},

$$\Theta_{ij} = \beta_0 + \beta_{\text{site}(i)} + \beta_{tr\,|\,\text{site}(ij)} + \beta_{gh} I(i), \tag{1}$$

which is a combination of the global trait mean (β_0), a normal random effect for study site ($\beta_{\text{site}(i)}$; i.e., accounts for spatial influence of topography, soil, etc.), a nested normal random effect for any experimental treatments ($\beta_{tr\,|\,\text{site}(ij)}$; i.e., accounts for influence of temperature, nitrogen etc.), and a fixed effect for greenhouse studies (β_{gh}; LeBauer et al., 2013). The term $I(i)$ is an indicator variable set to 0 for field studies and 1 for studies conducted in a greenhouse, growth chamber, or pot experiment. The posterior median for β_0 is the nominal parameter value input to ED2 and subsequently varied according to the posterior distribution of β_0 to perform the sensitivity and ensemble analysis. PEcAn uses JAGS software version 2.2.0 (Plummer, 2010) to fit equation (1). During the fitting procedure the Markov Chain Monte Carlo (MCMC) chains (4 per parameter) were tested for convergence according to the Gelman-Brooks-Rubin convergence criteria (Gelman & Rubin, 1992). More details on the linear mixed model and the fitting procedure can be found in LeBauer et al. (2013) and Text S4.

Two separate posterior distributions were calculated for this analysis, the first included the random effect terms when solving equation (1) (*posterior_re*) and the other excluded the random effects (*posterior*). Both the *posterior_re* and *posterior* distributions were calculated from the identical trait observations from the BETY database. The difference in the distributions arise from the effect of excluding the random effect terms in equation (1) ($\beta_{\text{site}(i)} = 0$, $\beta_{tr\,|\,\text{site}(ij)} = 0$), which assumes that all the trait observations were taken from the same population. The metric used to quantify parameter uncertainty is the *coefficient of variation* (CV), defined as the posterior standard deviation divided by the posterior mean (CV).

2.5.2. Calculating Parameter Sensitivity and Contribution to Model Uncertainty

The parameter distributions (section 2.5.1) were sampled to design a series of ED2 simulations to estimate the parameter contribution to model output uncertainty (e.g., mean, standard error, and credible interval). Specifically, ED2 was evaluated at ±(1,2,3) σ quantiles of the parameter being analyzed with all other parameters held at their nominal values listed in Table 1. The parameter uncertainty was transformed into the model uncertainty by fitting a cubic polynomial function (spline), g_p, to the model output. The partial variance, or fraction of the total variance contributed by parameter p, is estimated as

$$\text{partial variance}_p = \frac{\text{Var}\left[g_p\left(\beta_{o_p}\right)\right]}{\Sigma_{p=1}^{m}\text{Var}\left[g_p\left(\beta_{o_p}\right)\right]}, \tag{2}$$

where Var represents the variance operator, m is the total number of parameters that were varied, g is the fitted spline function, and β_o is the Monte Carlo sample of parameter values (based upon the parameter distribution (section 2.5.1) at which the spline is evaluated. The partial variance depends on both the parameter uncertainty (CV) and also the model elasticity (sensitivity of model to changes in a parameter). The elasticity is calculated as the derivative of g_p evaluated at the median parameter value, then multiplied by the parameter median over the model output median.

This partial variance calculation is a univariate approach and does not account for the interaction between parameters. Therefore, parameter interactions were calculated separately following LeBauer et al. (2013) in which the *ensemble* variance and the univariate estimate of variance are related by

$$\text{Var}[f(\boldsymbol{\beta_o})] = \Sigma_{p=1}^{m}\text{Var}\left[g_p\left(\beta_{o_p}\right)\right] + \omega. \tag{3}$$

Equation (3) states that the ensemble variance is equal to the sum of the parameter-specific univariate variances and a parameter interaction term ω. The ensemble (multivariate) variance was calculated by varying all parameters simultaneously to generate an ensemble of ED2 simulations. The sampling of the parameter distributions to create the ensemble used standard Monte Carlo techniques and was performed independently; therefore, there were no correlation between parameters. In practice, the computational expense of the ED2 model limited the number of ensemble members. The minimum number of members required to quantify the total variance was estimated by evaluating the ensemble variance as a function of the number of ensemble members. We conducted 200 ensemble runs as it exceeded the threshold beyond which the ensemble variance reached a constant value. Additional details about the multivariate variance calculation are located in Text S5.

2.5.3. Identifying Parameter Interactions

We used parameter interactions to identify the remaining parameters that significantly contributed to model uncertainty and were not identified within the univariate sensitivity analysis (section 2.5.2). Although equation (3) can identify the presence of interactions, it cannot identify specific parameter combinations responsible for the interaction. Therefore, we tested for specific pairs of parameters that interact by performing a filtered ensemble analysis (e.g., Knutti et al., 2002; Sriver et al., 2012). First, for every parameter combination a scatter plot was populated from the normalized parameter values defined by the ensemble. Second, parameter combinations were removed that led to model output outside the bounds of the NEE and AGB observations. Third, parameters were considered to interact if the filtered parameter pairs were significantly correlated.

The observations used to filter the parameter values were the average NEE from 2000 to 2005 as calculated by aggregated flux tower data (Ricciuto et al., 2013) and contemporary remotely sensed biomass data (Kellndorfer et al., 2012). Remotely sensed biomass data were chosen instead of plot-level, allometric-based biomass estimates because it was more consistent with the spatial region from the witness tree data and likely provided a more realistic estimate of biomass variability. The observed mean biomass at *US-WCr* was estimated from the average biomass of the 3×3 km^2 region composed of 30×30 m^2 grid cells surrounding the *US-WCr* forest stand. The acceptable range in the average biomass was estimated by the variation in the 1×1 km^2 subgrid regions. Following Barr et al. (2009) the uncertainty of the NEE was estimated by accounting for uncertainty from (1) limited sampling of turbulent eddies, (2) the choice of friction velocity filtering threshold, and (3) the gap-filling algorithm for missing flux data.

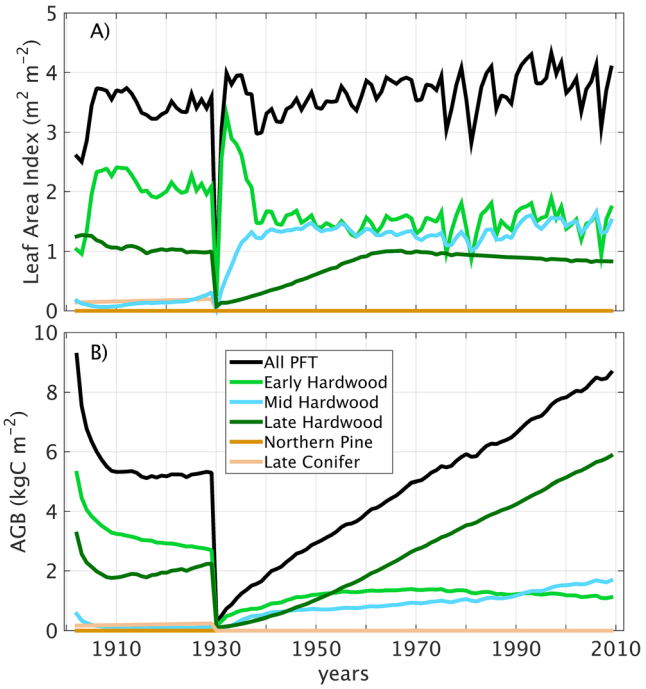

Figure 2. The simulation at *US-WCr* (using the median parameter values provided in Table 1) for (a) leaf area index and (b) aboveground biomass (AGB). The sharp drop at the year 1930 represents the prescribed logging event performed to mimic the actual management history of this site.

2.5.4. Implementing the Uncertainty Analysis at Willow Creek (*US-WCr*)

All simulations were run from June 1901 to January 2010, with initial vegetation conditions defined by the witness tree data (section 2.3) and atmospheric conditions (section 2.4). In accordance with site disturbance history, a clear-cut harvest was imposed within the model during the spring of 1930 by removing all AGB, and 99% of the belowground biomass. The removal of the belowground biomass was necessary to avoid unrealistic and vigorous resprouting of the forest immediately after the clear-cut. All of the harvested biomass was removed from the site and did not contribute to soil carbon or carbon emissions.

The contribution of model parameter uncertainty to the model uncertainty was evaluated by performing an uncertainty attribution analysis (sections 2.5.2 and 2.5.3) for model outputs of NEE, NPP, and AGB. The parameter contribution to model uncertainty was evaluated for short (1935–1940), middle (1935–70), and long (1935–2009) time frames of the model output. For simplicity these are referred to as annual, decadal, and centennial time frames, respectively, hereafter. These time frames were chosen to capture the growth and succession behavior after the imposed clear-cut of 1930.

For this analysis all conifer, early, and mid hardwood PFT parameters were fixed to their median values, and only the 15 late hardwood PFT parameters were allowed to vary across their parameter distributions. It was hypothesized that the overall forest stand dynamics at *US-WCr* is most sensitive to the late successional PFT given that this PFT dominates the present-day forest. This was also done to reduce the computational expense because each PFT had a separate parameter set.

This analysis was repeated for three separate parameter distributions: (1) prior, (2) *posterior*, and (3) *posterior_re*. The prior distributions used no trait data, only including the prior knowledge of the parameter distribution from the BETY database (Dietze, Serbin, et al., 2014). The *posterior* and *posterior_re* distributions include assimilated trait data through the Bayesian approach (section 2.5.1). If trait data were not available for a parameter, the prior distribution was used for all distributions. Unless otherwise noted, the *posterior_re* is the default within the results and discussion, and we discuss how this methodology influenced the results (section 4.3). In addition to the Bayesian approach, we performed manual hand adjustments to the *quantum efficiency* and *carbon balance mortality* parameter distributions to improve model agreement with contemporary observations (Figure 2). More information about the *US-WCr* observations can be found in Table S2 (Cook et al., 2008; Curtis et al., 2002). The parameter distributions for quantum efficiency for the late hardwood PFT (prior, *posterior,* and *posterior_re*) were tuned such that the median value increased from 0.045 to 0.06 μmol CO_2/(μmol photon) and the CV was kept the same. The nominal values for the carbon balance mortality for the early and middle hardwood PFTs were decreased from 20 year^{-1} to 3.5 and 7.0 year^{-1}, respectively. More details and justification for the manual tuning are provided in Text S6 (Davis, 2003; Singsaas et al., 2001).

For clarity and consistency when discussing elements of the sensitivity analysis, the uncertainty in the parameter values are referred to as parameter uncertainty (*estimated by CV*), the inherent model response to changes in a parameter is referred to as *sensitivity (estimated by elasticity),* and the variation in model output is referred to as model uncertainty *(estimated by partial variance)*.

3. Results and Discussion

3.1. Prior and Posterior Parameter Uncertainty

The late hardwood PFT parameter distribution for the prior, *posterior,* and *posterior_re* are described in Table 2 and Figure 3. Trait data were available for the meta-analysis for 5 out of the 15 parameters: *root/leaf carbon, specific leaf area, leaf respiration,* V_{cmax}, and *quantum efficiency*. The reduction in parameter spread (CI range)

Table 2
Parameter Distributions (posterior_re) for the Late Hardwood PFT as Shown in Figure 3 as Used in the Sensitivity Analysis

Parameters	Distribution (*a*,*b*)	*a*	*b*	N	Median	Lower bound	Upper bound
Carbon balance mortality	Gamma	1.47	0.0578	-	20.0	1.75	82.3
Root turnover	Weibull	1.55	0.862	-	0.49	0.053	0.94
Growth respiration	Beta	4.06	7.20	-	0.351	0.12	0.65
Stomatal sensitivity	Lognormal	1.76	0.38	-	5.84	2.73	12.4
Root/leaf carbon	Gamma	8.75	7.89	2	1.47	0.412	2.52
Reproduction carbon	Beta	2.00	3.00	-	0.312	0.046	0.72
Labile carbon	Beta	1.50	1.50	-	0.49	0.053	0.94
Soil-plant water cond.	Log normal	−5.40	3.00	-	0.00474	1.2e−05	2.17
Background mortality	Uniform	0.00	0.02	-	0.001	5.1e−04	0.02
Specific leaf area	Normal	16.6	2.24	88	16.6	10.3	22.8
Leaf respiration	Weibull	2.72	1.86	44	1.97	0.33	3.61
Quantum efficiency	Gamma	4.46	59.7	13	0.06	0.02	0.22
V_{cmax}	Normal	44.8	15.2	22	44.8	2.48	87.1
Root respiration	Weibull	2.00	10.00	-	8.31	1.37	19.3
Minimum height	Gamma	1.50	0.20	-	5.00	0.48	24.8

Note. The values *a* and *b* define the constants of the distribution function (LeBauer et al., 2014) for each parameter used in the sensitivity analysis. The sample size (*N*) is the number of mean trait observations used in the meta-analysis. Where trait data were not available, the parameter distributions were defined as the prior (Figure 3). The 95% credible interval (lower bound, upper bound) for each parameter is provided. The parameter units are provided in Table 1.

between the prior and *posterior_re* was 70%, 77%, 82%, 62%, and 47%, respectively, whereas the prior to posterior reduction in spread was much greater (97%, 99%, 99%, 97%, and 98%).

3.2. Model Output Uncertainty

The ensemble spread of all model output was strongly dependent upon the parameter distribution (Figure 4) where the CI range decreased in order from prior to *posterior_re* to *posterior*. The 95% confidence interval of

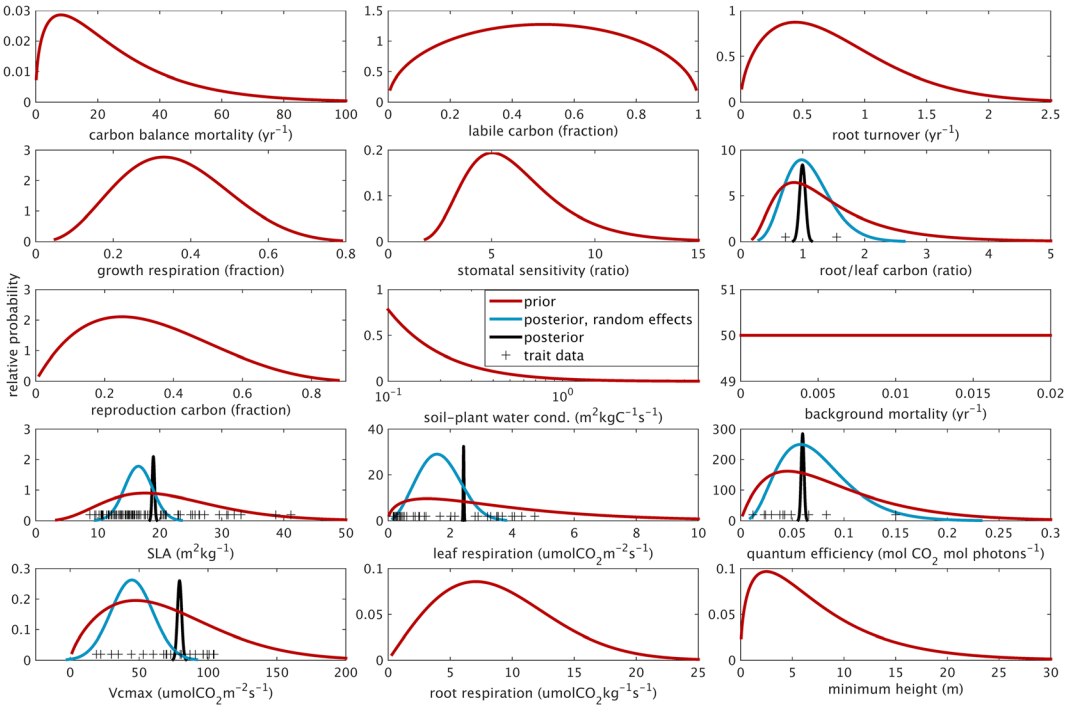

Figure 3. Parameter distributions for the late successional plant functional type. The prior distributions were taken from the BETY database (section 2.5.1) and were relatively broad. A Bayesian meta-analysis was performed to combine the posterior distributions with trait data (when available) to create *posterior* and *posterior_re* (includes random effects) distributions. These parameter distributions were used to estimate both the parameter and model uncertainty.

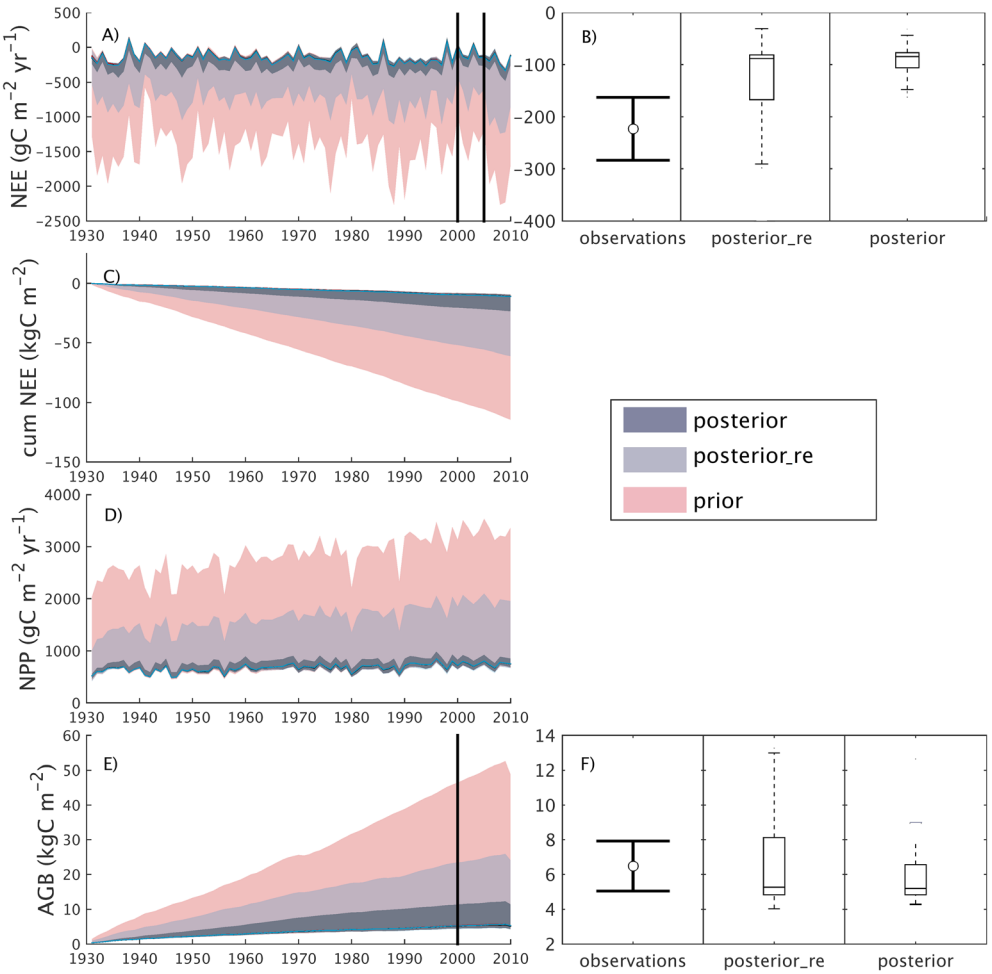

Figure 4. The 95% confidence intervals (shaded region) for the model output ensemble spread for the prior, *posterior_re*, and *posterior* parameter distributions for (a) net ecosystem exchange (NEE), (c) cumulative NEE, (d) net primary production (NPP), and (e) aboveground biomass (AGB). (b and f) Observations are for the 2000–2005 mean NEE (± 2σ), and 2000 AGB (± 2σ). The model simulation ensemble spread for the same time period respectively (vertical lines in panels a and e) is represented with box (25%, median, and 75% quartiles) and whisker (95% CI) plots (panels b and f). Negative NEE values represent a carbon sink to the land.

the ensemble prior ranged from 101 to 1,471 gC m^{-2} year^{-1} for NEE, 616–2,834 gC m^{-2} year^{-1} for NPP, and 4–48 kgC m^{-2} for AGB. The CI ranges reduced by 48%, 42%, and 70% from the prior to the *posterior_re* ensemble and by 80%, 72%, and 76% from the prior to *posterior* ensemble for NEE, NPP, and AGB, respectively.

3.3. Ecosystem Process Parameters that Contribute Most to Model Uncertainty

The model uncertainty based upon the *posterior_re* parameter distribution was dominated by the influence of the quantum efficiency, leaf respiration, and soil-plant water conductance (Figure 5). Overall this led to model uncertainty contributions of 40%, 18%, and 13% for *quantum efficiency, leaf respiration, and soil-plant water conductance,* respectively, for centennial NEE (Figure 6). Furthermore, the results of the uncertainty analysis based on the *posterior_re* distribution were similar regardless of model output (NEE, NPP, and AGB) and time frame (annual, decadal, and centennial; Figure 7). When parameter uncertainty was estimated by the *posterior* distribution, however, the parameters contributing the most to model uncertainty for centennial NEE were *soil-plant water conductance* (37%), *reproduction carbon* (24%), and *growth respiration* (20%). These parameters were the most important regardless of time or model output, although the relative order of importance shifted (Figures 6 and 7). Next, we discuss why these parameters contributed highly to uncertainty and how to reduce that contribution.

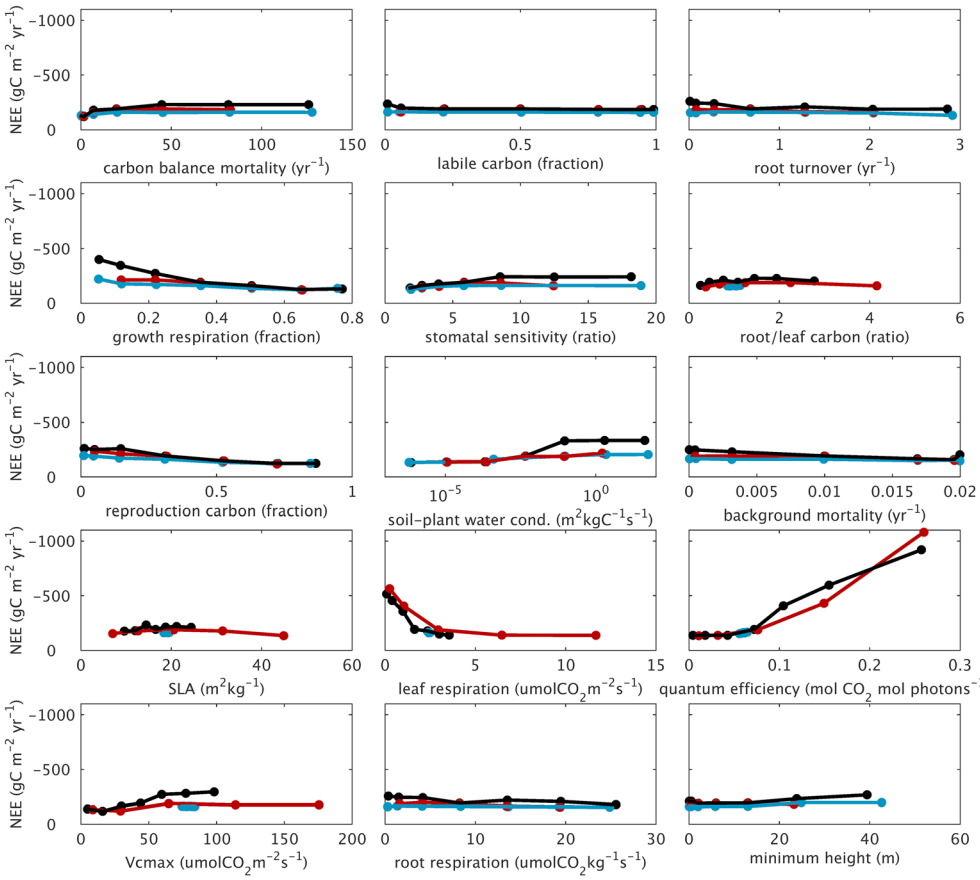

Figure 5. The response of model simulated net ecosystem exchange (NEE; 1935–2009 average; negative value = carbon sink) to parameter uncertainty according to the prior distribution (red), posterior distribution with random effects (*posterior_re*, blue), and posterior distribution without random effects (*posterior*, black). The model was evaluated at the median; ±1, 2 σ quantiles for the prior distribution and the median, and ±1, 2, 3 σ quantiles for the posterior distributions. The evaluated model response is fitted with a spline function for each parameter.

The high contribution of *quantum efficiency* and *leaf respiration* to model uncertainty was from a combination of high CV and elasticity (Figure 6). Although each parameter was subject to constraint by 13 and 44 sources of trait data respectively (Table 2), the effective sample size for reducing the parameter uncertainty was much lower (four and seven total sites, respectively). Therefore, the parameter uncertainty within the random effects model (i.e., within-site, across site, treatment, and greenhouse parameters) remained poorly constrained (Table S3). *Leaf respiration* is a fundamental physiological process tied to leaf cellular maintenance, while the *quantum efficiency* describes the initial slope of the relationship of photosynthesis to light and regulates the rate of carbon uptake under subsaturating conditions, and varies substantially across TBMs (Rogers et al., 2017). More field observations of these traits should be made a priority because they fundamentally control the leaf exchange of CO_2, are present in almost all TBMs (Rogers et al., 2017), and can be measured simultaneously using direct, leaf level photosynthetic light response curves.

The *soil–plant water conductance* parameter contributed the next most to model uncertainty in part because there was no trait data to reduce parameter uncertainty (Figure 3; i.e., not a directly observable trait). Assimilation of tower-based latent heat fluxes has the potential to inform the water conductance parameter; however, this is a weak constraint because tower-based latent heat fluxes do not distinguish between evaporation and canopy transpiration (Medvigy et al., 2009). Sap flux is a direct measure of stem transpiration and would likely provide a better constraint (Dietze, Serbin, et al., 2014); however, given the formulation in ED2, this approach also requires well-constrained estimates of LAI, stomatal slope, soil moisture, and fine root biomass. A better approach to representing water stress is to implement a hydraulic conductance model (Sperry & Love, 2015), thereby eliminating the need for an overall water conductance parameter. Hydraulic

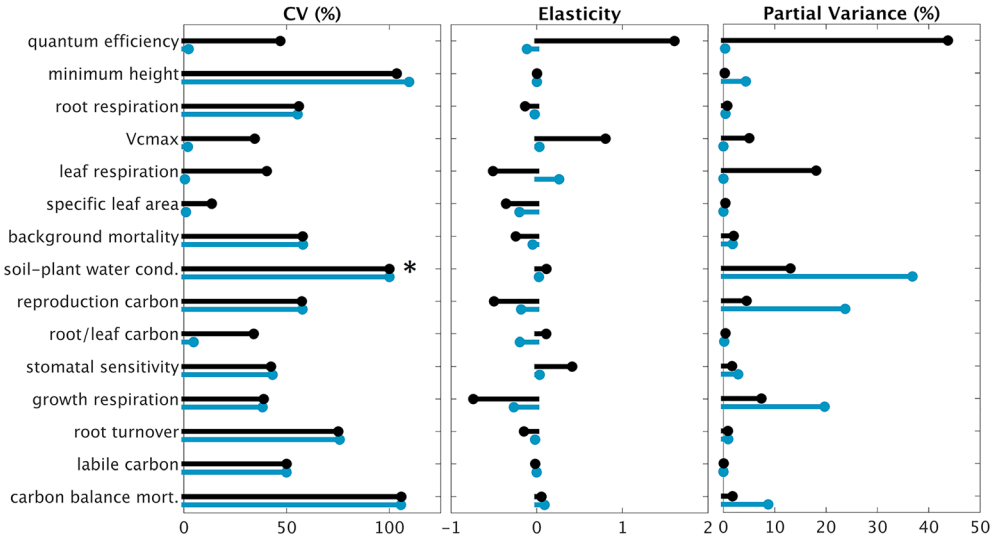

Figure 6. The parameter contribution to centennial-time scale model uncertainty (1935–2009 average net ecosystem exchange [NEE]) described in terms of (left panel) parameter uncertainty (coefficient of variation [CV]), (middle panel) model sensitivity (elasticity), and (right panel) model uncertainty (partial variance) for the *posterior_re* distribution (blue) and *posterior* distribution (black), respectively. The *asterisk* indicates that the *soil-plant water conductance* CV ($1.7 * 10^6$%) was displayed to 100 for better viewing of all parameters.

conductance models explicitly simulate water supply to the leaf through plant trait measurements (e.g., conductance across plant tissues and water potential at reduced conductivity). Such a model has been included in a recent update to ED2 (Xu et al., 2016) and could be constrained with existing databases for hydraulic traits (Bartlett et al., 2016; Choat et al., 2012).

The *reproduction carbon* parameter is also not directly observable and needs to be inferred from recruitment rate observations, which are difficult to find. Within ED2, the observed recruitment rate is a function of both the allocation of carbon to reproduction and a composite loss rate that combines seed and seedling mortality along with nonseed reproductive allocation (e.g., flowers, nectar, and pollen), which are highly conceptualized (nonmechanistic) parameters. For this analysis the loss rate was fixed at 95% because the correlation (equifinality) between these two parameters makes it challenging to constrain each individually. In a more recent implementation of ED2, the seedling mortality of aspen and black spruce was constrained by growth trends and germination experiments with mortality increasing with organic layer depth (Trugman et al., 2016). In general, a more detailed model representation of the processes that control the carbon allocated to reproduction, seed dispersal, and sapling survival is needed and an active topic of research (e.g., Clark et al., 2012; Schupp & Jordano, 2011). A particularly important question is to what degree large-scale models need to represent distance- and density-dependent mechanisms of mortality that go beyond carbon balance, such as seed and seedling predation and disease, which have long been thought to play a large role in population stability and the maintenance of biodiversity (Bagchi et al., 2014; Dietze & Matthes, 2014; Janzen, 1970).

The *growth respiration* parameter is challenging to estimate as it is represents the overall building cost from a variety of plant tissues (Medvigy et al., 2009). A more detailed approach to represent growth respiration is through a pathway analysis approach (Penning de Vries et al., 1974) which accounts for the fact that biosynthesis costs are dependent upon the type of biochemical compounds (i.e., protein, carbohydrates, lipids, lignin, and organic acids) and their abundance in different plant tissues (e.g., leaf, stem, and root). This approach is being implemented in PEcAn; however, a significant bottleneck is that plant trait databases need more plant tissue composition data to make use of the additional mechanistic complexity.

We found no compelling evidence that parameter interactions significantly altered the evaluation of important parameters in this analysis. The >50% reduction between the ensemble variance and sum of the univariate variance (Table S4) demonstrated significant parameter interaction; however, this was not surprising given that ED2 is a mechanistically detailed and nonlinear model. The bivariate approach (section 2.5.3)

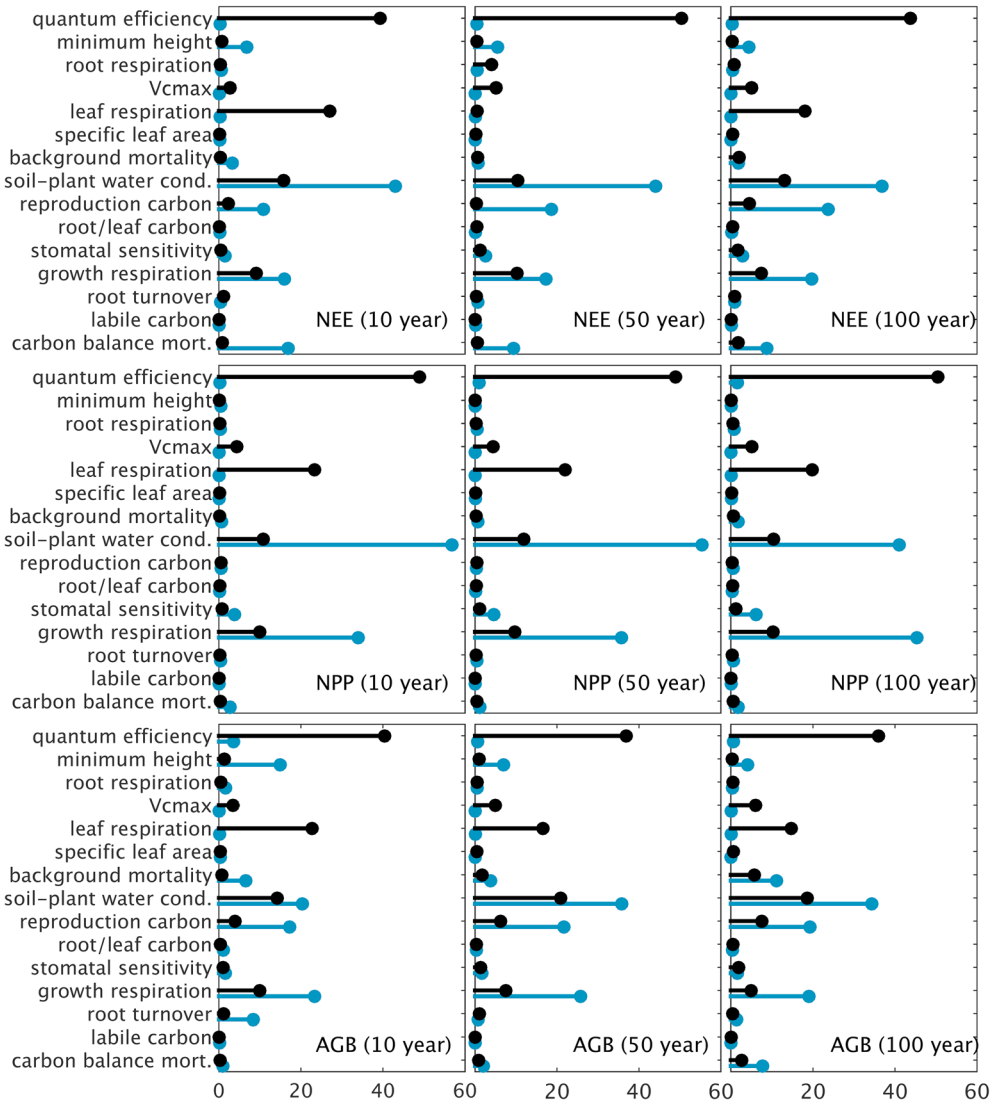

Figure 7. The relative contribution of ecological parameters to model uncertainty (partial variances) based upon the *posterior_re* (blue) and *posterior* (black) distributions for net ecosystem exchange (NEE), net primary production (NPP), and aboveground biomass (AGB) averaged for different time scales: 10 year = 1935–1940, 50 year = 1935–1970, and 100 year = 1935–2009.

identified overall weak parameter correlations given 8% and 4% of all possible parameter combinations was correlated to 95% certainty for NEE and NEE/AGB filtering, respectively (Figures S3 and S4). We expected 5% of the parameters to have correlation purely by chance alone, suggesting interactions played a minimal role on the results.

4. Discussion

4.1. Ecosystem Processes Contributing to Carbon Uptake Uncertainty

An uncertainty attribution analysis was performed within a cohort-based TBM (ED2) to understand what ecological processes contribute the most to carbon uptake uncertainty. Whereas previous analyses focused upon relatively short-term (<20 years) carbon dynamics (e.g., Dietze, Serbin, et al., 2014) or a single time frame (e.g., Pappas et al., 2013; Ricciuto et al., 2018), here we focused on multiple time frames (annual, multidecadal, and centennial). For this analysis, the expectation was that fast physiological parameters (e.g., V_{cmax}, *quantum efficiency, leaf respiration,* and *stomatal sensitivity*) were expected to dominate the carbon dynamic uncertainty for short time scales, whereas parameters that control successional processes and the ecosystem state (e.g.,

Table 3
Top Parameter Contributors to Uncertainty Based Upon Partial Variance Analysis for Net Primary Productivity (NPP; <10 years)

Raczka NPP (*posterior_re*)	Raczka NPP (*posterior*)	(Dietze, Serbin, et al., 2014) NPP (posterior, no random effects)
Quantum efficiency (50%)	*Soil-plant water cond.* (>50%)	*Growth respiration* (>50%)
Leaf respiration (25%)	*Growth respiration* (28%)	*Soil-plant water cond.* (11%)
Soil-plant water cond. (12%)	*Stomatal sensitivity* (5%)	*Stomatal sensitivity* (10%)
Growth respiration (12%)	*Carbon balance mort.* (3%)	*Quantum efficiency* (7%)
		Carbon balance mort. (6%)

Note. Dietze, Serbin, et al. (2014) values are based upon the average contribution across all hardwood plant functional type (PFT) sites.

mortality parameters and *reproduction carbon*) were expected to be more important at the centennial time scale. Instead, we found that parameters related to the fast physiological response including *quantum efficiency, leaf respiration, soil–plant water conductance,* and *growth respiration* contributed the most to carbon uptake regardless of the time frame. This finding that fast-response parameters controlled the carbon dynamics was generally consistent with previous short-term ED2 uncertainty analyses performed at multiple biomes (Dietze, Serbin, et al., 2014), poplar (Wang et al., 2013) and switchgrass (LeBauer et al., 2013; Tables 3 and 4). The only ecosystem parameter within this study associated with long-term successional processes and model state and contributed significantly to model uncertainty was *reproduction carbon;* however, it never accounted for more than 10% of the model uncertainty (Figure 7).

Other sensitivity analyses performed across multiple sites and PFTs identified processes related to photosynthesis to be the most impactful upon carbon dynamics. For example, the most influential parameters were related to V_{cmax} for the Community Land Model (CLM; Sargsyan et al., 2014), V_{cmax} and maintenance respiration for the Energy Exascale Earth System Model (E3SM; Ricciuto et al., 2018), V_{cmax} and *quantum efficiency* for the Australian community land model (CABLE; Lu et al., 2013), and intrinsic quantum efficiency for the Luna-Potsdam-Jena General Ecosystem Simulation Model (LPJ-GUESS; Pappas et al., 2013). Similar to ED2, LPJ-GUESS is a cohort-based gap model capable of simulating competition and successional processes, yet similar to our study, fast response physiological responses dominated. Importantly, the findings were similar even though Pappas et al. (2013) used uniform priors, whereas our study used more informative prior and posterior parameter distributions based on trait data. This suggests that the parameter uncertainty in our analysis remained relatively broad despite the trait database. We discuss reasons for this in section 4.2.

The influence of successional processes upon long-term carbon dynamics could have been masked by across-PFT parameter interactions. For example, the fact that processes related to mortality (e.g., carbon balance and density independent mortality) were not critical for the development of the overall forest dynamics may have resulted from compensating effects between the early and mid hardwood PFTs. High mortality for the late hardwood PFT discourages growth for that PFT; however, this should increase resource availability (e.g., sunlight) and promote growth for the competing PFTs, providing minimal net change to the forest stand overall. This compensating effect may explain why the simulated NEE was relatively consistent regardless of the PFT composition (Figures 2 and 4). The influence of across-PFT parameter interactions was not identified here because late hardwood PFT parameters were varied and model uncertainty was based upon total stand composition (all PFTs). Across-PFT interactions could be better isolated by (1) performing an across-PFT sensitivity analysis (Saltelli et al., 2008) upon a more limited set of parameters for each PFT or

Table 4
Top Parameter Contributors to Uncertainty Based Upon Partial Variance Analysis for Above Ground Biomass (AGB; <10 years)

Raczka AGB (*posterior_re*)	Raczka AGB (*posterior*)	(Wang et al., 2013) AGB (poplar)	(LeBauer et al., 2013) AGB (switchgrass)
Quantum efficiency (40%)	*Growth resp.* (>50%)	*Growth resp.*	*Growth resp.* (12%)
Leaf respiration (25%)	*Water cond.* (28%)	*Leaf resp.*	*Root/leaf carbon* (10%)
Water cond. (15%)	*Minimum height* (23%)	*Quantum effic.*	*Leaf turnover* (7%)
Growth resp. (10%)	*Rep. alloc.* (5%)	*Carbon mortality*	*Specific leaf area* (5%)
		Water cond.	

Note. The plant functional type (PFT) type is variable across this comparison where Raczka = late hardwood PFT, Wang = poplar only (no random effects), and LeBauer = switchgrass only (no random effects). The *soil-plant water conductance* parameter is abbreviated with *water conductance*.

(2) basing the sensitivity analysis on % composition variables of NEE, AGB, or NPP instead of total stand composition as was done here.

The secondary importance of mortality upon the ecosystem state could have reflected limitations within the model. The version of ED2 used in this analysis calculated the carbon balance mortality as a function of carbon balance based on light competition, ignoring any contribution to mortality from hydraulic limitation (drought mortality). Finding observations to inform the carbon balance mortality rate, however, is challenging given the long life span of trees (Dietze & Moorcroft, 2011) and the difficulties in directly measuring the carbon balance of trees in the field (Dietze, Sala, et al., 2014; Mantooth, 2017).

4.2. Impact of Random Effects Upon Parameter and Model Uncertainty

Including random effects to estimate parameter uncertainty made a significant impact upon the relative contribution of ecosystem process to model uncertainty (Figure 7). Excluding random effects replaced *quantum efficiency* and *leaf respiration* with *soil–plant water conductance* and *growth respiration* as the parameters that most influence model uncertainty, which was more consistent with previous ED2 analyses (e.g., Dietze, Serbin, et al., 2014; LeBauer et al., 2013; Wang et al., 2013). Unlike these previous uncertainty analyses, we chose to include random effects (*posterior_re*) because excluding them led to unrealistically narrow posterior distributions and led to simulations inconsistent with observations (Figure 4b). Furthermore, assuming trait data is drawn from the same distribution (i.e., no random effects) may underestimate the true variability of the parameters and therefore provide an overconfident estimate of model uncertainty (Dietze, 2017a). Considering random effects, however, makes it necessary to estimate additional parameters within equation (1) (e.g., across-site precision, Table S4) using data from multiple study sites. For example, four out of the five parameters that were calibrated with trait data had between 13 and 88 observations (sample mean for a particular species, site, and treatment); however, the number of unique sites from which the trait data were measured was much less (range from 5 to 10 sites per trait). The availability of trait data also dictates the level of specificity for the PFT. In this analysis PFTs were defined by successional stage; however, with additional trait data the PFTs could be made species specific (i.e., maple, basswood, and ironwood) potentially reducing the parameter uncertainty.

Beyond just the availability of trait data, the parameter uncertainty is also related to the TBM representation of an ecosystem process. Whereas a portion of the parameter uncertainty is reducible through trait data, a portion is irreducible and represents missing processes within the modeling system (process error; Dietze, 2017b). Future work should pay close attention how an expanding trait database combined with increasingly mechanistic representation of ecosystem process impact the posterior parameter distributions.

As an alternative to quantifying random effects through trait databases, the site-to-site variability captured by random effects can also be estimated as part of Hierarchical Bayesian calibration approaches (Dietze, 2017a), which have recently been implemented in PEcAn (Fer et al., 2018). Future studies should estimate the parameter variability and quantify the impact upon model uncertainty through this calibration approach.

4.3. Experimental Design Improvements

This analysis focused upon the impact of aboveground ecosystem processes, whereas a more comprehensive uncertainty analysis should include the impact of belowground carbon cycling processes, aboveground and belowground initial conditions, and atmospheric forcing (Dietze, 2017b). Preliminary simulations suggest that ED2 is highly sensitive to both the representation and initialization of soil carbon processes given that different methodologies in initializing the soil carbon pools (i.e., initializing from observations versus spinning up from bareground state) led to significant differences in carbon uptake (Figure S5). A more recent version of PEcAn includes belowground carbon cycling parameters and the capability to treat initial conditions as an adjustable parameter within the uncertainty analysis.

This analysis used a univariate parameter approach coupled with an ad-hoc bivariate correlation analysis to estimate first and second order (interactions) parameter effects upon model uncertainty. The relatively large number of parameters and computational expense of the model prevented a more formal variance based sensitivity approach. However, the elementary effects approach (i.e., method of Morris) combined with a Sobol' sensitivity analysis (e.g., Saltelli et al., 2008) has the capability to filter out unimportant parameters and directly quantify first-order, second-order, and total-order sensitivity indices. Approaches such as these

could help expand the analysis to early, middle, and late hardwood PFTs and quantify across-PFT interactions, which we hypothesized to be important (section 4.1).

Parameters were assumed independent in this analysis, but information about parameter correlations should be included to help reduce parameter uncertainty. A more recent version of PEcAn included an estimate of parameter correlations both within and across PFTs for seven leaf traits (Shiklomanov et al., 2018). They found that including covariance within multivariate modeling reduced the mean trait uncertainty; however, across-PFT correlations added little additional constraint to the model outcome. It would be worth expanding this beyond leaf traits to include interactions amongst successional processes as well.

5. Conclusions

We have performed an uncertainty analysis within a cohort-based TBM with a representation of processes important to plant-based succession including reproduction, resource competition, and mortality. The expectation was for successional processes to become increasingly important to the simulated carbon uptake and overall model state as simulation time increased from annual to multidecadal to centennial time frames. Against expectations, we found that parameters most responsible for fast physiological response including *quantum efficiency, leaf respiration,* and *soil–plant water conductance* were most influential upon carbon dynamics regardless of the simulation time. This was in part because the parameter uncertainty was relatively large for these processes driven by a significant variation in trait data across different sites and treatment conditions. These findings suggest the most efficient approach to reducing model predictive uncertainty is through a more exhaustive search for trait-level data to reduce *quantum efficiency* and *leaf respiration* uncertainty and reduce the variety of species within a PFT. The *soil-plant water conductance* parameter, on the other hand, is highly empirical and hard to constrain in demographic models (Fisher et al., 2018); therefore, we recommend a restructuring of the model formulation to allow for direct measurements of the hydraulic processes that are fundamental to water transfer. These finding were based upon a univariate uncertainty approach and limited to primarily aboveground ecosystem processes. A more comprehensive uncertainty analysis should consider the importance of across-PFT interactions for succession based processes, and the influence of belowground carbon cycling processes.

Data Availability

ED-2 source code can be found at https://github.com/EDmodel/ED2. PEcAn source code is located at https://github.com/PecanProject/pecan. Plant trait data is located within the BETY database at https://www.betydb.org/. Meteorological and biological data for the Ameriflux site Willow Creek (*US-WCr*) are available at http://ameriflux.lbl.gov/sites/siteinfo/US-WCr. Witness tree data can be found through Liu et al. (2011), and remotely sensed biomass data are available through Kellndorfer et al. (2012).

Acknowledgments
This work was supported by the National Institute for Climatic Change Research (NICCR) as part of the Terrestrial Ecosystem Science (TES) program managed by the U.S. Department of Energy's Office of Biological and Environmental Research (BER). M. Dietze and PEcAn development were supported by NSF ABI 1062547 and 1458021 and NSF DIBBs 1261582 and S. Serbin was partially supported by NSF ABI 1062547 as well as the U.S. Department of Energy contract DE-SC0012704 to Brookhaven National Laboratory. We are grateful to David LeBauer for helpful discussions and support related to the functioning of ED2, PEcAn, and BETY. We would also like to thank Ryan Knox for developing ED2 output visualization software and Doug Baldwin for providing assistance with remotely sensed biomass data. Travel to the University of Illinois was funded by the National Science Foundation through an INTERFACE Student Exchange Travel Grant. Finally, thank you to IT services at Penn State and the University of Illinois.

References

Arora, V. K., Boer, G. J., Friedlingstein, P., Eby, M., Jones, C. D., Christian, J. R., et al. (2013). Carbon-concentration and carbon-climate feedbacks in CMIP5 Earth System Models. *Journal of Climate*, *26*(15), 5289–5314. https://doi.org/10.1175/JCLI-D-12-00494.1

Bagchi, R., Gallery, R. E., Gripenberg, S., Gurr, S. J., Narayan, L., Addis, C. E., et al. (2014). Pathogens and insect herbivores drive rainforest plant diversity and composition. *Nature*, *506*(7486), 85–88. https://doi.org/10.1038/nature12911

Ball, J. T., Woodrow, I. E., & Berry, J. A. (1987). A model predicting stomatal conductance and its contribution to the control of photosynthesis under different environmental conditions. In J. Biggins (Ed.), *Progress in Photosynthesis Research* (pp. 221–224). Netherlands: Springer. https://doi.org/10.1007/978-94-017-0519-6_48

Barr, A. G., Hollinger, D., & Richardson, A. D. (2009). CO_2 flux measurement uncertainty estimates for NACP, Eos Trans. AGU, 90(52), fall meet. Suppl., abstract B54A-04.

Bartlett, M. K., Klein, T., Jansen, S., Choat, B., & Sack, L. (2016). The correlations and sequence of plant stomatal, hydraulic, and wilting responses to drought. *Proceedings of the National Academy of Sciences*, *113*(46), 13,098–13,103. https://doi.org/10.1073/pnas.1604088113

Bauer, G. A., Berntson, G. M., & Bazzaz, F. A. (2001). Regenerating temperate forests under elevated CO_2 and nitrogen deposition: Comparing biochemical and stomatal limitation of photosynthesis. *New Phytologist*, *152*(2), 249–266. https://doi.org/10.1046/j.0028-646X.2001.00255.x

Bolker, B. M., Pacala, S. W., & Parton, W. J. (1998). Linear analysis of soil decomposition: Insights from the century model. *Ecological Applications*, *8*(2), 425–439. https://doi.org/10.1890/1051-0761(1998)008[0425:LAOSDI]2.0.CO;2

Botta, A., Viovy, N., Ciais, P., Friedlingstein, P., & Monfray, P. (2000). A global prognostic scheme of leaf onset using satellite data. *Global Change Biology*, *6*(7), 709–725. https://doi.org/10.1046/j.1365-2486.2000.00362.x

Braswell, B. H., Sacks, W. J., Linder, E., & Schimel, D. S. (2005). Estimating diurnal to annual ecosystem parameters by synthesis of a carbon flux model with eddy covariance net ecosystem exchange observations. *Global Change Biology*, *11*(2), 335–355. https://doi.org/10.1111/j.1365-2486.2005.00897.x

Caswell, H. (2001). *Matrix population models* (Second). Sunderland, Massachusetts: Sinaurer Associates.
Choat, B., Jansen, S., Brodribb, T. J., Cochard, H., Delzon, S., Bhaskar, R., et al. (2012). Global convergence in the vulnerability of forests to drought. *Nature*, *491*(7426), 752–755. https://doi.org/10.1038/nature11688
Clark, J. S., Soltoff, B. D., Powell, A. S., & Read, Q. D. (2012). Evidence from individual inference for high-dimensional coexistence: Long-term experiments on recruitment response. *PLoS One*, *7*(2), e30050. https://doi.org/10.1371/journal.pone.0030050
Cook, B. D., Davis, K. J., Wang, W. G., Desai, A., Berger, B. W., Teclaw, R. M., et al. (2004). Carbon exchange and venting anomalies in an upland deciduous forest in northern Wisconsin, USA. *Agricultural and Forest Meteorology*, *126*(3–4), 271–295. https://doi.org/10.1016/j.agrformet.2004.06.008
Cook, B. D., Bolstad, P. V., Martin, J. G., Heinsch, F. A., Davis, K. J., Wang, W., et al. (2008). Using light-use and production efficiency models to predict photosynthesis and net carbon exchange during Forest canopy disturbance. *Ecosystems*, *11*(1), 26–44. https://doi.org/10.1007/s10021-007-9105-0
Curtis, P. S., Hanson, P. J., Bolstad, P., Barford, C., Randolph, J. C., Schmid, H. P., & Wilson, K. B. (2002). Biometric and eddy-covariance based estimates of annual carbon storage in five eastern North American deciduous forests. *Agricultural and Forest Meteorology*, *113*(1-4), 3–19. https://doi.org/10.1016/S0168-1923(02)00099-0
Davidson, C. D. (2012). The modeled effects of fire on carbon balance and vegetation abundance in Alaskan tundra. M.S. Thesis, University of Illinois, Urbana-Champaign.
Davis, K. J. (2003). *Well-calibrated CO_2 mixing ratio measurements at flux towers: The virtual tall towers approach, (161), 101–108.*
Desai, A. R., Bolstad, P. V., Cook, B. D., Davis, K. J., & Carey, E. V. (2005). Comparing net ecosystem exchange of carbon dioxide between an old-growth and mature forest in the upper Midwest, USA. *Agricultural and Forest Meteorology*, *128*(1–2), 33–55. https://doi.org/10.1016/j.agrformet.2004.09.005
Dietze, M. C. (2017a). *Ecological forecasting*. Princeton, NJ: Princeton University Press. https://doi.org/10.1515/9781400885459
Dietze, M. C. (2017b). Prediction in ecology: A first-principles framework. *Ecological Applications*, *27*(7), 2048–2060. https://doi.org/10.1002/eap.1589
Dietze, M. C., Lebauer, D. S., & Kooper, R. (2013). On improving the communication between models and data. *Plant, Cell & Environment*, *36*(9), 1575–1585. https://doi.org/10.1111/pce.12043
Dietze, M. C., & Matthes, J. H. (2014). A general ecophysiological framework for modelling the impact of pests and pathogens on forest ecosystems. *Ecology Letters*, *17*(11), 1418–1426. https://doi.org/10.1111/ele.12345
Dietze, M. C., & Moorcroft, P. R. (2011). Tree mortality in the eastern and central United States: Patterns and drivers. *Global Change Biology*, *17*(11), 3312–3326. https://doi.org/10.1111/j.1365-2486.2011.02477.x
Dietze, M. C., Sala, A., Carbone, M. S., Czimczik, C. I., Mantooth, J. A., Richardson, A. D., & Vargas, R. (2014). Nonstructural carbon in woody plants. *Annual Review of Plant Biology*, *65*(1), 667–687. https://doi.org/10.1146/annurev-arplant-050213-040054
Dietze, M. C., Serbin, S. P., Davidson, C., Desai, A. R., Feng, X., Kelly, R., et al. (2014). A quantitative assessment of a terrestrial biosphere model's data needs across North American biomes. *Journal of Geophysical Research: Biogeosciences*, *119*, 286–300. https://doi.org/10.1002/2013JG002392
Etheridge, D. M., Steele, L. P., Langenfelds, R. L., Francey, R. J., Barnola, J. M., & Morgan, V. I. (1998). Historical CO_2 records from the Law Dome DE08, DE08-2, and DSS ice cores. In Trends: A Compendium of Data on Global Change. Carbon Dioxide Information Analysis Center, Oak Ridge National Laboratory, U.S. Department of Energy, Oak Ridge, Tenn., U.S.A.
Farquhar, G. D., von Caemmerer, S., & Berry, J. A. (1980). A biochemical model of photosynthetic CO2 assimilation in leaves of C3 species. *Planta*, *149*(1), 78–90. https://doi.org/10.1007/BF00386231
Fer, I., Kelly, R., Moorcroft, P. R., Richardson, A. D., Cowdery, E. M., & Dietze, M. C. (2018). Linking big models to big data: Efficient ecosystem model calibration through Bayesian model emulation. *Biogeosciences Discussions*, *2018*, 1–30. https://doi.org/10.5194/bg-2018-96
Fisher, R. A., Koven, C. D., Anderegg, W. R. L., Christoffersen, B. O., Dietze, M. C., Farrior, C. E., et al. (2018). Vegetation demographics in Earth System Models: A review of progress and priorities. *Global Change Biology*, *24*(1), 35–54. https://doi.org/10.1111/gcb.13910
Franco, M., & Silvertown, J. (1996). Life history variation in plants: An exploration of the fast-slow continuum hypothesis. *Philosophical Transactions of the Royal Society of London B: Biological Sciences*, *351*(1345), 1341–1348. https://doi.org/10.1098/rstb.1996.0117
Friedlingstein, P., Meinshausen, M., Arora, V. K., Jones, C. D., Anav, A., Liddicoat, S. K., & Knutti, R. (2014). Uncertainties in CMIP5 climate projections due to carbon cycle feedbacks. *Journal of Climate*, *27*(2), 511–526. https://doi.org/10.1175/JCLI-D-12-00579.1
Gelman, A., & Rubin, D. B. (1992). Inference from iterative simulation using multiple sequences. *Statistical Science*, *7*(4), 457–472. https://doi.org/10.1214/ss/1177011136
Janzen, D. H. (1970). Herbivores and the number of tree species in tropical forests. *American Naturalist*, *104*(940), 501–528. https://doi.org/10.1086/282687
Jose, S., & Gillespie, A. (1996). Aboveground production efficiency and canopy nutrient contents of mixed-hardwood forest communities along a moisture gradient in the central United States. *Canadian Journal of Forest Research*, *26*(12), 2214–2223. https://doi.org/10.1139/x26-250
Keenan, T. f., Baker, I., Barr, A., Ciais, P., Davis, K., Dietze, M., et al. (2012). Terrestrial biosphere model performance for inter-annual variability of land-atmosphere CO2 exchange. *Global Change Biology*, *18*(6), 1971–1987. https://doi.org/10.1111/j.1365-2486.2012.02678.x
Kellndorfer, J., Walker, J., LaPoint, E., Bishop, J., Cormier, T., Fiske, G., et al. (2012). NACP aboveground biomass and carbon baseline data (NBCD 2000), U.S.a., 2000. Data set. Available on-line at http://daac.ornl.gov from ORNL DAAC, Oak Ridge, Tennessee, U.S.A. https://doi.org/10.3334/ORNLDAAC/1081
Knutti, R., Stocker, T. F., Joos, F., & Plattner, G. K. (2002). Constraints on radiative forcing and future climate change from observations and climate model ensembles. *Nature*, *416*(6882), 719–723. https://doi.org/10.1038/416719a
LeBauer, D. S., Dietze, M. C., & Bolker, B. M. (2014). Translating probability density functions: From R to BUGS and back again. *The R Journal*, *5*(1), 207–209.
LeBauer, D. S., Wang, D., Richter, K. T., Davidson, C. C., & Dietze, M. C. (2013). Facilitating feedbacks between field measurements and ecosystem models. *Ecological Monographs*, *83*(2), 133–154. https://doi.org/10.1890/12-0137.1
Le Quéré, C. L., Andrew, R. M., Friedlingstein, P., Sitch, S., Pongratz, J., Manning, A. C., et al. (2018). Global carbon budget 2017. *Earth System Science Data*, *10*(1), 405–448. https://doi.org/10.5194/essd-10-405-2018
Leuning, R. (1995). A critical appraisal of a combined stomatal-photosynthesis model for C3 plants. *Plant, Cell & Environment*, *18*(4), 339–355. https://doi.org/10.1111/j.1365-3040.1995.tb00370.x
Levin, S. A., Grenfell, B., Hastings, A., & Perelson, A. S. (1997). Mathematical and computational challenges in population biology and ecosystems science. *Science*, *275*(5298), 334–343. https://doi.org/10.1126/science.275.5298.334

Lin, J. C., Pejam, M. R., Chan, E., Wofsy, S. C., Gottlieb, E. W., Margolis, H. A., & McCaughey, J. H. (2011). Attributing uncertainties in simulated biospheric carbon fluxes to different error sources. *Global Biogeochemical Cycles*, *25*, GB2018. https://doi.org/10.1029/2010GB003884

Liu, F., Mladenoff, D. J., Keuler, N. S., & Moore, L. S. (2011). Broadscale variability in tree data of the historical Public Land Survey and its consequences for ecological studies. *Ecological Monographs*, *81*(2), 259–275. https://doi.org/10.1890/10-0232.1

Lu, X., Wang, Y.-P., Ziehn, T., & Dai, Y. (2013). An efficient method for global parameter sensitivity analysis and its applications to the Australian community land surface model (CABLE). *Agricultural and Forest Meteorology*, *182–183*, 292–303. https://doi.org/10.1016/j.agrformet.2013.04.003

Mantooth, J. (2017). Tree radial growth and carbohydrate storage in eastern US temperate forest. PhD Dissertation. Department of Earth & Environment, Boston University.

Medvigy, D., Wofsy, S. C., Munger, J. W., Hollinger, D. Y., Moorcroft, P., & R. (2009). Mechanistic scaling of ecosystem function and dynamics in space and time: Ecosystem demography model version 2. *Journal of Geophysical Research*, *114*, G01002. https://doi.org/10.1029/2008JG000812

Medvigy, David. (2006). The state of the regional carbon cycle: Results from a coupled constrained ecosystem-atmosphere model, (PhD thesis). Cambridge, MA: Harvard University.

Medvigy, D., & Moorcroft, P. R. (2012). Predicting ecosystem dynamics at regional scales: An evaluation of a terrestrial biosphere model for the forests of northeastern North America. *Philosophical Transactions of the Royal Society of London B: Biological Sciences*, *367*(1586), 222–235. https://doi.org/10.1098/rstb.2011.0253

Moorcroft, P. R., Hurtt, G. C., & Pacala, S. W. (2001). A method for scaling vegetation dynamics: The ecosystem demography model (ed). *Ecological Monographs*, *71*(4), 557–586. https://doi.org/10.1890/0012-9615(2001)071[0557:AMFSVD]2.0.CO;2

Pacala, S. W., & Deutschman, D. H. (1995). Details that matter: The spatial distribution of individual trees maintains Forest ecosystem function. *Oikos*, *74*(3), 357–365. https://doi.org/10.2307/3545980

Pappas, C., Fatichi, S., Leuzinger, S., Wolf, A., & Burlando, P. (2013). Sensitivity analysis of a process-based ecosystem model: Pinpointing parameterization and structural issues. *Journal of Geophysical Research: Biogeosciences*, *118*, 505–528. https://doi.org/10.1002/jgrg.20035

Parton, W., Stewart, J., & Cole, C. (1988). Dynamics of C, N, P And S in grassland soils—A model. *Biogeochemistry*, *5*(1), 109–131. https://doi.org/10.1007/BF02180320

Penning de Vries, F., Brunsting, A., & Van Laar, H. (1974). Products, requirements and efficiency of biosynthesis: A quantitative approach. *Journal of Theoretical Biology*, *45*(2), 339–377. https://doi.org/10.1016/0022-5193(74)90119-2

Plummer, M. (2010). JAGS (just another Gibbs sampler). Version 2.2.0 user manual. http://ftp.jaist.ac.jp/pub/sourceforge/m/project/mc/mcmc-jags/Manuals/2.x/jags_user_manual.pdf

Raczka, B. M., Davis, K. J., Huntzinger, D., Neilson, R. P., Poulter, B., Richardson, A. D., et al. (2013). Evaluation of continental carbon cycle simulations with North American flux tower observations. *Ecological Monographs*, *83*(4), 531–556. https://doi.org/10.1890/12-0893.1

Ricciuto, D., Sargsyan, K., & Thornton, P. (2018). The impact of parametric uncertainties on biogeochemistry in the E3SM land model. *Journal of Advances in Modeling Earth Systems*, *10*(2), 297–319. https://doi.org/10.1002/2017MS000962

Ricciuto, D. M., Butler, M. P., Davis, K. J., Cook, B. D., Bakwin, P. S., Andrews, A., & Teclaw, R. M. (2008). Causes of interannual variability in ecosystem-atmosphere CO2 exchange in a northern Wisconsin forest using a Bayesian model calibration. *Agricultural and Forest Meteorology*, *148*(2), 309–327. https://doi.org/10.1016/j.agrformet.2007.08.007

Ricciuto, D. M., Schaefer, K., Thornton, P. E., Davis, K. J., Cook, R. B., Liu, S., et al. (2013). NACP site: Terrestrial biosphere model and aggregated flux data in standard format. Data set. Available on-line [http://daac.ornl.gov] from oak Ridge National Laboratory distributed active archive center, oak ridge, Tennessee, USA. https://doi.org/10.3334/ORNLDAAC/1183

Ricciuto, D. M., King, A. W., Dragoni, D., & Post, W. M. (2011). Parameter and prediction uncertainty in an optimized terrestrial carbon cycle model: Effects of constraining variables and data record length. *Journal of Geophysical Research*, *116*, G01033. https://doi.org/10.1029/2010JG001400

Richardson, A. D., Williams, M., Hollinger, D. Y., Moore, D. J. P., Dail, D. B., Davidson, E. A., et al. (2010). Estimating parameters of a forest ecosystem C model with measurements of stocks and fluxes as joint constraints. *Oecologia*, *164*(1), 25–40. https://doi.org/10.1007/s00442-010-1628-y

Rogers, A., Medlyn, B. E., Dukes, J. S., Bonan, G., von Caemmerer, S., Dietze, M. C., et al. (2017). A roadmap for improving the representation of photosynthesis in Earth system models. *New Phytologist*, *213*(1), 22–42. https://doi.org/10.1111/nph.14283

Saltelli, A., Ratto, M., Andres, T., Campolongo, F., Cariboni, J., Gatelli, D., et al. (2008). *Global Sensitivity Analysis, The Primer*. Chichester, UK: John Wiley.

Saltelli, A., Tarantola, S., & Campolongo, F. (2000). Sensitivity analysis as an ingredient of modeling. *Statistical Science*, *15*(4), 377–395.

Sargsyan, K., Safta, C., Najm, H. N., Debusschere, B. J., Ricciuto, D., & Thornton, P. (2014). Dimensionality reduction for complex models via bayesian compressive sensing. *International Journal for Uncertainty Quantification*, *4*(1), 63–93. https://doi.org/10.1615/Int.J.UncertaintyQuantification.2013006821

Schimel, D., Pavlick, R., Fisher, J. B., Asner, G. P., Saatchi, S., Townsend, P., et al. (2015). Observing terrestrial ecosystems and the carbon cycle from space. *Global Change Biology*, *21*(5), 1762–1776. https://doi.org/10.1111/gcb.12822

Schupp, E. W., & Jordano, P. (2011). The full path of Janzen-Connell effects: Genetic tracking of seeds to adult plant recruitment. *Molecular Ecology*, *20*(19), 3953–3955. https://doi.org/10.1111/j.1365-294X.2011.05202.x

Schwalm, C. R., Williams, C. A., Schaefer, K., Anderson, R., Arain, M. A., Baker, I., et al. (2010). A model-data intercomparison of CO_2 exchange across North America: Results from the North American Carbon Program site synthesis. *Journal of Geophysical Research*, *115*, G00H05. https://doi.org/10.1029/2009JG001229

Shiklomanov, A. N., Cowdery, E. M., Bahn, M., Byun, C., Jansen, S., Kramer, K., et al. (2018). Does the leaf economic spectrum hold within plant functional types? A Bayesian multivariate trait meta-analysis. *BioRxiv*, 475038. https://doi.org/10.1101/475038

Shugart, H. H., Asner, G. P., Fischer, R., Huth, A., Knapp, N., Le Toan, T., & Shuman, J. K. (2015). Computer and remote-sensing infrastructure to enhance large-scale testing of individual-based forest models. *Frontiers in Ecology and the Environment*, *13*(9), 503–511. https://doi.org/10.1890/140327

Singsaas, E. L., Ort, D. R., & DeLucia, E. H. (2001). Variation in measured values of photosynthetic quantum yield in ecophysiological studies. *Oecologia*, *128*(1), 15–23. https://doi.org/10.1007/s004420000624

Sperry, J. S., & Love, D. M. (2015). What plant hydraulics can tell us about responses to climate-change droughts. *New Phytologist*, *207*(1), 14–27. https://doi.org/10.1111/nph.13354

Sriver, R., Urban, N., Olson, R., & Keller, K. (2012). Toward a physically plausible upper bound of sea-level rise projections. *Climatic Change*, *115*(3-4), 893–902. https://doi.org/10.1007/s10584-012-0610-6

Tang, J., Bolstad, P. V., & Martin, J. G. (2009). Soil carbon fluxes and stocks in a Great Lakes forest chronosequence. *Global Change Biology*, *15*(1), 145–155. https://doi.org/10.1111/j.1365-2486.2008.01741.x

Thoning, K. W., Tans, P. P., & Komhyr, W. D. (1989). Atmospheric carbon dioxide at Mauna Loa Observatory 2. Analysis of the NOAA GMCC data, 1974-1985. *Journal of Geophysical Research*, *94*, 8549–8565. https://doi.org/10.1029/JD094iD06p08549

Trugman, A. T., Fenton, N. J., Bergeron, Y., Xu, X., Welp, L. R., & Medvigy, D. (2016). Climate, soil organic layer, and nitrogen jointly drive forest development after fire in the North American boreal zone. *Journal of Advances in Modeling Earth Systems*, *8*, 1180–1209. https://doi.org/10.1002/2015MS000576

Walko, R. L., Band, L. E., Baron, J., Kittel, T. G. F., Lammers, R., Lee, T. J., et al. (2000). Coupled atmosphere–biophysics–hydrology models for environmental modeling. *Journal of Applied Meteorology*, *39*(6), 931–944. https://doi.org/10.1175/1520-0450(2000)039<0931:CABHMF>2.0.CO;2

Walters, M. B., Kruger, E. L., & Reich, P. B. (1993). Relative growth rate in relation to physiological and morphological traits for northern hardwood tree seedlings: Species, light environment and ontogenetic considerations. *Oecologia*, *96*(2), 219–231. https://doi.org/10.1007/BF00317735

Wang, D., LeBauer, D., & Dietze, M. (2013). Predicting yields of short-rotation hybrid poplar (Populus spp.) for the United States through model–data synthesis. *Ecological Applications*, *23*(4), 944–958. https://doi.org/10.1890/12-0854.1

Weiss, A., & Norman, J. M. (1985). Partitioning solar radiation into direct and diffuse, visible and near-infrared components. *Agricultural and Forest Meteorology*, *34*(2-3), 205–213. https://doi.org/10.1016/0168-1923(85)90020-6

Weng, E. S., & Luo, Y. Q. (2011). Relative information contributions of model vs. data to short- and long-term forecasts of forest carbon dynamics. *Ecological Applications*, *21*(5), 1490–1505. https://doi.org/10.1890/09-1394.1

Woods, K. D. (2000). Dynamics in late-successional hemlock–hardwood forests over three decades. *Ecology*, *81*(1), 110–126. https://doi.org/10.1890/0012-9658(2000)081[0110:DILSHH]2.0.CO;2

Xu, X., Medvigy, D., Powers, J. S., Becknell, J. M., & Guan, K. (2016). Diversity in plant hydraulic traits explains seasonal and inter-annual variations of vegetation dynamics in seasonally dry tropical forests. *New Phytologist*, *212*(1), 80–95. https://doi.org/10.1111/nph.14009